Biosensors and Bioelectronics 26 (2011) 2177–2182

Contents lists available at ScienceDirect

Biosensors and Bioelectronics

journal homepage: www.elsevier.com/locate/bios

An amperometric biosensor based on rat cytochrome p450 1A1 for benzo[a]pyrene determination

Yunhua Wu*, Xuequn Liu, Li Zhang, Chuntai Wang

Key Lab for Biotechnology of National Commission for Nationalities, College of Life Science, South Central University for Nationalities, Wuhan 430074, PR China

ARTICLE INFO

Article history:
Received 22 July 2010
Received in revised form 1 September 2010
Accepted 15 September 2010
Available online 22 September 2010

Keywords:
Cytochrome P450 1A1
Escherichia coli
Benzo[a]pyrene
Cyclic voltammetry
Biosensor

ABSTRACT

Using the plasmid pCW, high-level expression of rat cytochrome p4501A1 (CYP1A1) has been achieved by making NH_2-terminal translational fusions to bacterial leader sequences *ompA* (ompA-1A1/pCW). The construct ompA-1A1 was compared with an expression construct in which the Ala codon GCT was placed in the second position and 5′-terminal codons were maximized for A T content (1A1/pCW). Both constructs produced spectrally active, functional protein. However, the ompA-1A1 fusion gave higher levels of expression, and a marked improvement in the recovery of active P450 in bacterial membrane fractions, when compared with the construct 1A1/pCW. The expressed 1A1 from the construct ompA-1A1/pCW in bacterial membrane fractions were collected and immobilized in nano-Na-montmorillonite (nano-SWy-2) and dihexadecylphosphate (DHP) composite film. The direct electrochemistry of CYP1A1 in a nano-SWy-2-DHP film on an edge-plane pyrolytic graphite electrode (EPG) has been obtained and the catalytic activity of the enzyme to benzo[a]pyrene has been investigated by the cyclic voltammetry. The immobilized CYP1A1 displayed a pair of redox peaks with a formal potential of −0.36 mV in pH 7.0 O_2-free phosphate buffers at scan rate of 1 V s^{-1}. The CYP1A1 in the nano-SWy-2-DHP film retained its bioactivity and could catalyze the reduction of dissolved oxygen. Upon the addition of its substrate benzo[a]pyrene (B[a]P) to the air-saturated solution, the reduction peak current of dissolved oxygen increased, which indicates the catalytic behavior of CYP1A1 to B[a]P. By amperometry a calibration linear range for B[a]P was obtained to be 3.31–16.56 μM with a sensitivity of 58.57 μA mM^{-1}. And the apparent Michaelis–Menten constant for the electrocatalytic activity of CYP1A1 was estimated to be 46.27 μM for B[a]P.

1. Introduction

Cytochrome P450 (CYP) enzymes catalyze oxidative metabolism of a wide array of endogenous and exogenous compounds, including many environmental contaminants. CYP-mediated metabolism can result in either detoxification or activation and can determine the persistence of some xenobiotics, thereby influencing their toxicity (Uno et al., 2006). CYP1A1, the best-known CYP member, is one of the major aryl hydrocarbon receptor (AhR)-sensitive targets and is highly induced by benzo[*a*]pyrene (B[a]P) (Shimada, 2006). It was reported that the B[a]P-induced CYP1A1 enzyme mediates B[a]P-induced toxicity (Solhaug et al., 2004; Chung et al., 2007). Therefore, CYP1A1, as a representative CYP, is widely used in studies of benzo[*a*]pyrene metabolism. CYP1A1 is associated with key steps in the oxidation of B[a]P, namely 7,8-epoxidation of B[a]P and 9,10-epoxidation of B[a]P-7,8-diol (Ji et al., 2007).

CYP1A1 is not expressed appreciably in human liver but lung (Pacifici and Fracchia, 1995). However, the enzyme isolated from human lung is not fully active (Shimada et al., 1992). In order to study B[a]P metabolism, it is necessary to develop high-level P450 expression systems to obtain sufficient amounts of P450s. Heterologous P450 expression systems have been proved to be very important in P450 biochemical research. Among several other expression systems, bacterial expression systems using *Escherichia coli* cells provide a number of advantages in terms of high yield, low cost, and ease of handling (Larson et al., 1991). The improved expression of a slightly 5′-terminus modified human p450 1A1 in *E. coli* was firstly reported in 1994 (Guo et al., 1994). After that, an enzymatically active fusion protein between the cDNA for human P450 1A1 and rat NADPH-P450 reductase was expressed in *E. coli* (Chun et al., 1996). The purified fusion protein can oxidize B[a]P in the absence of added NADPH-p450 reductase. To express high-level P450s, the approach has also been used by means of NH_2-terminal fusion to a bacterial signal peptide. This type of strategy has been used successfully for the heterologous expression of a number of recombinant proteins in *E. coli*, including human apolipoprotein E (Monteilhet et al., 1993) and human cytochrome P450 3A4 (Pritchard et al., 1997).

* Corresponding author. Tel.: +86 27 8750 6365; fax: +86 27 6784 2689.
E-mail address: yunhuawu@yahoo.com.cn (Y. Wu).

0956-5663/$ – see front matter © 2010 Elsevier B.V. All rights reserved.
doi:10.1016/j.bios.2010.09.027

B[a]P is a well-known environmental toxicant and a prototype of carcinogenic polycyclic aromatic hydrocarbons (PAHs) (Shimada, 2006). It is usually generated through the combustion of fossil fuels, wood, and other organic materials and is found in significant amounts in diesel exhaust, cigarette smoke, charcoal-broiled foods, and industrial waste by-products (Hecht, 1999). Because of their carcinogenic activity, considerable effort has been devoted to their analysis. Of the methods proposed for B[a]P analysis, the best developed was HPLC with UV (Akpan et al., 1994) or Fluorescence detection (Troche et al., 2000). Since B[a]P is the substrate of cytochrome p450 1A1, an enzyme biosensor based on cytochrome p450 1A1 can be developed for the B[a]P analysis. To show cytochrome p450 1A1 activity, a natural redox partner, NADPH cytochrome P450 reductase, is usually required *in vitro*. But for an electrochemical cytochrome p450s biosensor, no natural redox partner is required because an electrode directly supplies the electrons required to drive cytochrome p450s-mediated catalysis.

In this paper, two constructs of rat cDNA in the plasmid pCW with a modified 5′-terminus or NH_2-terminal fusion to a bacterial signal peptide *ompA* have been expressed in *Escherichia coli*. The level of expression in two constructs was compared and the *ompA* fusion gave higher levels of expression. The highly expressed rat cytochrome p450 1A1 was isolated from the bacterial membranes and immobilized in a nano-SWy-2-DHP film to develop a biosensor. The direct electrochemistry CYP1A1 in the nano-SWy-2-DHP film on an edge-plane pyrolytic graphite electrode (EPG) has been obtained and the catalytic activity of the enzyme to benzo[a]pyrene has been investigated by cyclic voltammetry and amperometry.

2. Materials and methods

2.1. Construction of expression plasmids

Total RNA was isolated from the lung of rat by the acid guanidinium–phenol–chloroform method (Trizol; Invitrogen). First-strand cDNA was synthesized with 4U Moloney murine leukemia virus (M-MLV) reverse transcriptase (Toyobo). Approximately 1 μg total RNA was combined with 10 pmol oligo(dT), 10 U RNase inhibitor, 0.1 mM dNTPs, 4 μL native 5× RT buffer in a total volume of 200 μL. Following incubation at 37 °C for 30 min, the reaction was heated to 99 °C for 5 min, and then placed on ice. At this point, the PCR primers (30 pmol of each) were added. The forward 5′-AGCGACATATGGCTTCTGTTTATGGATTTCCAGC-3′ (the underlined sequence is the NdeI site) and reverse 5′-GCAAAGCTTCTAAGCCTGGAGATGCTGAGGAC-3′ (the underlined sequence is the HindIII site) were synthesized as the primers. Creation of the NdeI site resulted in a change in the second coded amino acid residue in the wild-type sequence from Asp to Ala. Native KOD-Plus polymerase (1.25 U) and 10 μL with 10× KOD-Plus buffer were then added, and the incubation volume was made up to 100 μL with sterilized ddH_2O. PCR was carried out for 34 cycles and annealing at 57 °C. The resulting PCR product, of approximately 15 kb, was digested with NdeI and HindIII, purified using a spin column, and ligated into pCW (NdeI/HindIII cut). This construct was denoted as 1A1/pCW.

For the *ompA* fusion to the full-length CYP1A1, two-step PCR was employed according to the Ref. (Pritchard et al., 1997). The sequences of 5′ forward primer, the leader and the linker are as follows: 5′-GGAATTCCATATGAAAAAGACAGCTATCGCG-3′, 5′-ATGAAAAAGACAGCTATCGCGATTGCAGTGGCACTGGCTGGTTTCGC TACCGTAGCGCAGGCCGCTCCG-3′ and 5′-AGGCTGGGAATCCATA-CACAGAAGGCATCGGAGCGGCCTGCGCTACGGTAGCGAAACCA-3′, respectively. The final PCR product was ligated into pCW as described above, to produce the construct ompA-1A1/pCW.

2.2. Expression of recombinant protein and preparation of membranes

E. coli DH5α cells were made competent and transformed with each of the expression plasmids. Transformed cells were stored as 20% glycerol stocks at −80 °C. All experiments of the expression of recombinant protein and preparation of membranes were carried out as described previously (Zhang et al., 2010).

2.3. Characterization of CYP1A1 expression

The *E. coli* membranes were resuspended in 20 mM Tris–acetate buffer (pH 7.4) containing 0.25 mM EDTA and 0.25 M sucrose. Fe^{2+} vs. Fe^{2+}/CO difference spectra were measured according to Omura and Sato (Omura and Sato, 1964). CYP1A1 content was determined by using an extinction coefficient of 91 mM^{-1} cm^{-1}. Expression level of the enzyme was investigated visually by SDS-polyacrylamide gel electrophoresis.

2.4. Preparation of the modified electrode

The colloid of nano-SWy-2 was prepared by following steps (Yuan et al., 2004): 30 mg SWy-2 was thoroughly dispersed in 2 mL water by continuous stirring for 12 h, and then kept quiet for 5 h. The topper suspension was collected after centrifuging at 3500 rpm for 30 min. 10 mM DHP was dispersed in 4 mL *nano-SWy-2 colloid* or distilled water by ultrasonicating for 16 h until it was homogeneous and a *nano-SWy-2*-DHP or DHP aqueous dispersion was obtained. The active area of an edge-plane pyrolytic graphite electrode (EPG) with diameter 3 mm was determined by cyclic voltammmetry using the Randles–Sevcik equation for a reversible redox couple $[Fe(CN)_6]^{3-}/[Fe(CN)_6]^{2-}$ with a value about 2.08 cm^2. Prior to modification, the edge-plane pyrolytic graphite electrode was polished with 0.3 μm and 0.05 μm alumina slurry (CH instrument, INC.) in sequence, then sonicated in ethanol and doubly distilled water, respectively. CYP1A1 was dissolved in 50 mM phosphate buffer (pH 7.4) to achieve a concentration of 0.10 mM and this solution was mixed with an equal volume of the clear vesicle dispersions of DHP or *nano-SWy-2*-DHP. This mixed solution (5 μL) was cast onto the EPG and let water evaporated in air for 24 h. Thus, the total amount of the immobilized protein is 25 nmol (0.10 mM × 5 μL/2). The modified electrodes are denoted as CYP1A1-*nano-SWy-2*-DHP/EPG and CYP1A1-DHP/EPG, respectively in this paper.

2.5. Cyclic voltammetry

Cyclic voltammetry (CV) was performed with a CHI660C electrochemical workstation (CH Instruments, Shanghai, China). A three-electrode system, including a working CYP1A1 modified electrode, a saturated calomel electrode (SCE) and a platinum wire counter electrode, was employed. Prior to each experiment, the buffer solutions were purged with high-purity nitrogen for at least 30 min and a nitrogen environment was then kept over the solution in the cell. All experiments were carried out at room temperature.

3. Discussion and results

3.1. Expression of CYP1A1

An expression system for rat p450 1A1 in *E. coli* strain DH5α with the plasmid pCW was applied according to the reports that it was found to be successful for p450 enzymes expression (Sandhu et al., 1994; Pritchard et al., 1997). As mentioned above, two expression constructs for p450 1A1 were characterized in this study. Construct 1 (1A1/pCW) employed substitution of the second codon with GCT (Ala), resulting in amino acid changes within the p450

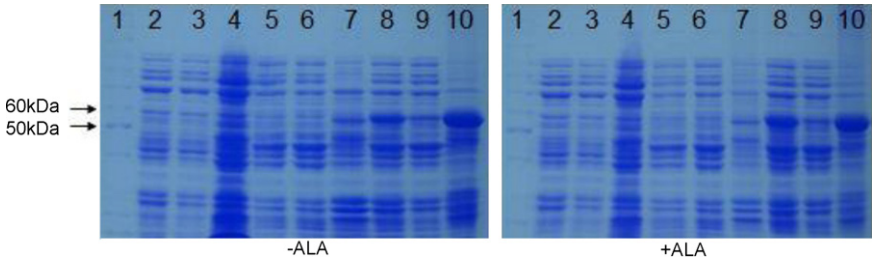

Fig. 1. Characterization the expression of recombinant P450 1A1 by SDS-PAGE in the presence (right) and absence (left) of exogenous δ-aminolevulinic acid. Lane 1: Molecular size markers; lane 2–4: the whole cell lysate, the supernatant of the whole cell lysate and the deposit of f the whole cell lysate of *E. coli*. with the pCW vector with a non-expressed insert, respectively; lane 5–7: the whole cell lysate, the supernatant of the whole cell lysate and the deposit of the whole cell lysate of *E. coli*. with the 1A1/pCW construct, respectively; lane 8–10: the whole cell lysate, the supernatant of the whole cell lysate and the deposit of the whole cell lysate of *E. coli*. with the ompA-1A1/pCW construct, respectively.

protein chain. Construct 2 contained *E. coli* leader sequence that encoded by part of the *ompA* gene, fused to full-length CYP1A1. The leader sequence was designed according to an *E. coli ompA* gene sequence submitted to the database (Accession No. v00307). *E. coli* DH5α freshly transformed with the indicated expression plasmids were cultured for 24 h at 32 °C and harvested as described in Zhang et al. (2010). To assay the expression level, the cells were broken by sonication, each fraction of cells (i.e. membranes and debris) was collected by different centrifugal speeds. Samples were loaded on a denaturing sodium dodecyl sulfate (SDS) gel on the basis of equal total amount of protein determined by the Lowry assay (Lowry et al., 1951), and the expression level was assessed by visual inspection. In the experiment the influence on the expression level with or without addition of δ-aminolevulinic acid (δ-ALA) was also investigated. Results are shown in Fig. 1. The recombinant protein is located at the band about 58,000 Da, which is not seen from *E. coli* containing the vector without an insert. It was found that construct 2 displayed enhanced expression yields compared to construct 1, i.e., the amount of recombinant protein produced was obvious to have been up-regulated significantly by the addition of a native *E. coli* signal sequence *ompA* to the gene. The large amount of expressed enzyme did produce fusion protein of the correct size as inclusion bodies.

To characterize and determine the CYP1A1 content, the method of Omura and Sato was used and the result was listed in Table 1. Consent with the result in Fig. 1, expression from ompA-1A1/pCW was markedly higher than that from 1A1/pCW construct, almost giving 300 nmol p450/l culture. Interesting, the addition of δ-ALA in the culture medium had little influence on the ompA-1A1/pCW construct. But to 1A1/pCW construct, no p450 can be detected without δ-ALA addition. The Fe^{2+}-CO vs. Fe^{2+} difference spectra obtained in both bacterial cells and membrane fractions are shown in Fig. 2, which shows a slightly small appearance of p420 peak, indicates the good quality of the recombinant protein being produced. The fraction of membrane-bound proteins was separated and solubilized by Triton N-101. The solubilized membrane-bound proteins were concentrated by ultrafiltration and the resulted enzyme aliquots were to be used to develop a CYP1A1 biosensor.

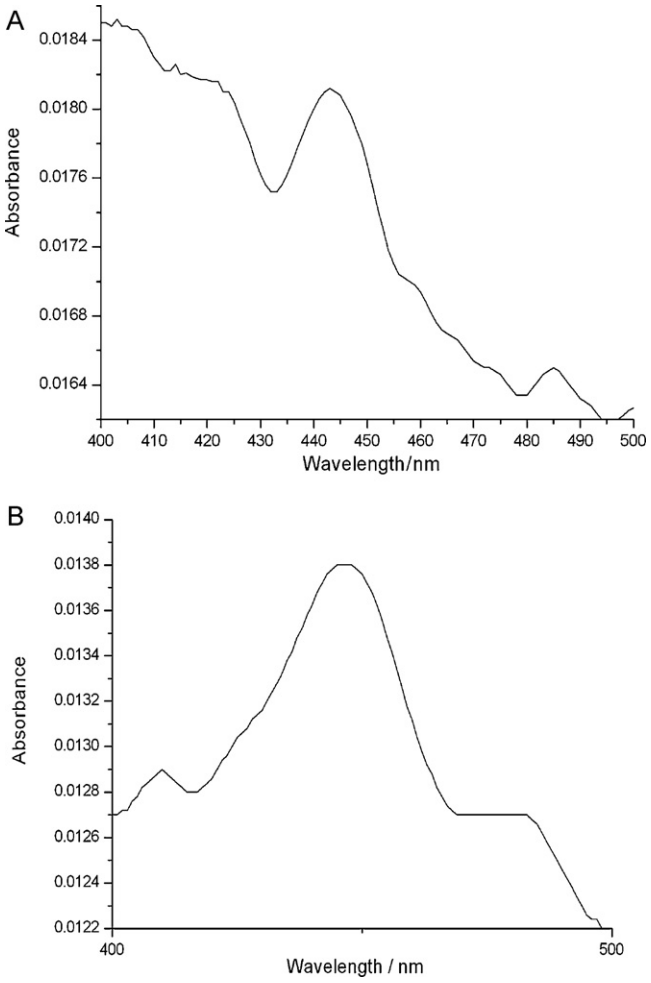

Fig. 2. Fe^{2+}-CO vs. Fe^{2+} difference spectra showing expression of CYP1A1 from the construct *ompA*-1A1/pCW in *E. coli* cells (A) and membranes (B). For spectral analysis, samples were diluted in 100 mM Tris–HCl pH 7.4, containing 20% glycerol (v/v), 10 mM Triton N-101, and 1 mM EDTA.

Table 1
Expression of CYP1A1 from different constructs in the presence and absence of δ-aminolevulinic acid.[a]

Construct	δ-ALA	Expression level Whole cells (nmol/150 mL culture)	Membranes (nmol/150 mL culture)	Membrane p450 content (nmol/mg protein)
1A1/pCW	–	nd	nd	nd
	+	19.13	13.72	15.7
OmpA-1A1/pCW	–	28	19.5	21.4
	+	43.08	34.68	46.3

nd: not be detected.
[a] Expression was carried out at 32 °C for 24 h in *E. coli* DH5α cells with 1.0 mM IPTG, with or without 0.5 mM δ-ALA.

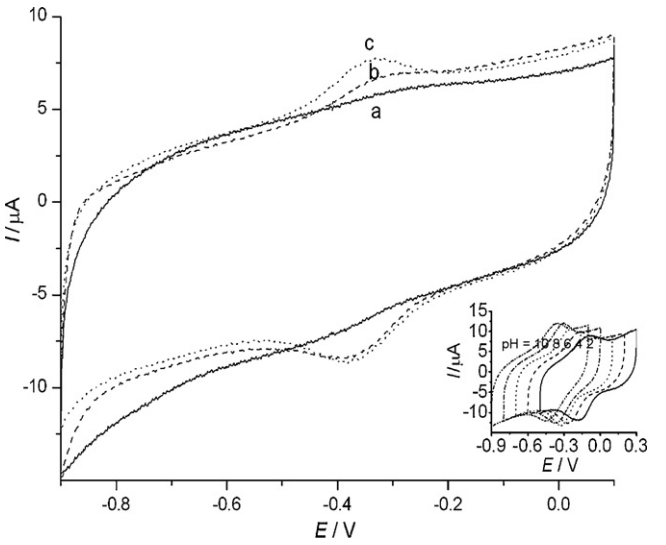

Fig. 3. Cyclic voltammograms at 1 V s^{-1} in oxygen-free pH 7.0 buffers for: nano-SWy-2-DHP/EPG (a); CYP1A1-DHP/EPG (b) and CYP1A1-nano-SWy-2-DHP/EPG (c). Inset: Cyclic voltammograms of CYP1A1-nano-SWy-2-DHP/EPG in different pH values with scan rate of 1 V s^{-1}.

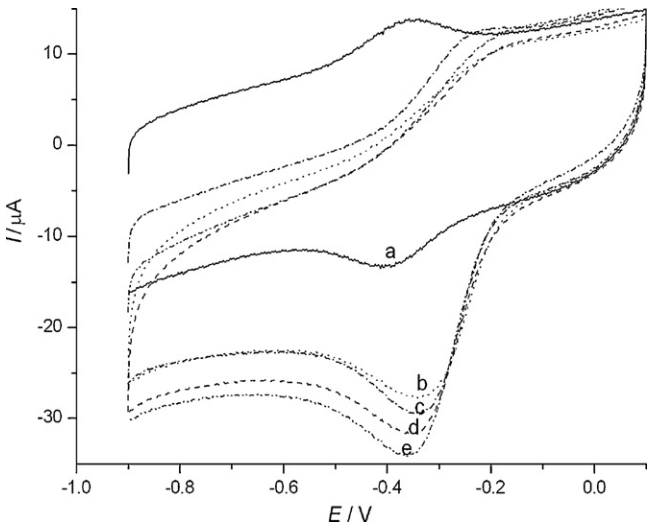

Fig. 4. Cyclic voltammograms of the CYP1A1-nano-SWy-2-DHP/EPG in the N_2-saturated buffer (a), in the air-saturated buffer (b), in the air-saturated buffer after addition of 3.32 μM (c); 6.64 μM (d) and 9.96 μM (e) benzo[*a*]pyrene at scan rate of 1 V s^{-1}, respectively.

3.2. Direct electrochemistry of CYP1A1 in nano-SWy-2-DHP film

Curve a–c in Fig. 3 shows the cyclic voltammograms (CVs) of a *nano-SWy-2*-DHP/EPG, a CYP1A1-DHP/EPG and CYP1A1-*nano-SWy-2*-DHP/EPG in pH 7.0 phosphate buffer at scan rate of 1 V s^{-1}, respectively. No any observable peak was obtained at the *nano-SWy-2*-DHP/EPG (curve a), but a pair of well-defined and stable peaks was observed at the CYP1A1-DHP/EPG, corresponding to the reaction of P-FeII/P-FeIII couple of CYP1A1 (curve b). It suggests that DHP can immobilize CYP1A1 and provides a favorable microenvironment to facilitate its direct electron transfer communication. However, when using *nano-SWy-2*-DHP to immobilize the same amount of CYP1A1, the peak currents increase obviously (curve c), indicating *nano-SWy-2*-DHP acts as an improved active interface for the direct electron transfer of CYP1A1. Clay nanoparticles have the advantages of high chemical stability, good adsorption property due to its appreciable surface area, and electrocatalytical ability. Clay has been used to realize the direct electron transfer of redox proteins, such as horseradish peroxidase (Zhao et al., 2008) and myoglobin (Zhou et al., 2002). The formal potential ($E_{0'}$) of CYP1A1 in *nano-SWy-2*-DHP film electrode is around −0.36 V and the peak potential separation (ΔE_p) is 40 mV at scan rate of 1 V s^{-1}.

CVs of CYP1A1-*nano-SWy-2*-DHP film had approximately symmetric peak shapes and nearly equal heights of reduction and oxidation peaks with scan rates in the range from 1 V s^{-1} to 10 V s^{-1}. At scan rates lower than 1 V s^{-1}, reduction current is higher than oxidation current because of residue oxygen in CYP1A1-*nano-SWy-2*-DHP film. Thus, 1 V s^{-1} was chosen in the following experiments. Reduction peak currents increased linearly with scan rates in the range from 1 V s^{-1} to 10 V s^{-1}. Integration of reduction peaks at different scan rates gave nearly constant charges (Q) values. All these are characteristic of surface-control electrochemical behavior (Murray, 1984). The surface coverage of the electroactive CYP1A1 (Γ) on CYP1A1-*nano-SWy-2*-DHP/EPG was estimated from integration of the reduction peak in the CVs according to $\Gamma = Q/nFA$, where Q is the charge involved in the reaction, n the number of electron transferred, F Faraday constant, and A the electrode area, with the result of 5.29×10^{-12} mol cm^{-2} for CYP1A1. These values are just about 5% or less of the total amount of protein coated on the electrode surface. This may suggest that only those enzymes in the inner layers of films closest to electrodes and with a suitable orientation can exchanges electrons with the electrodes and contribute to the observed redox reaction.

The kinetics of the heterogeneous electron transfer was analyzed using the model of Laviron (Laviron, 1979). For a peak separation <200 mV and the scan rate of 1 V s^{-1}, the electron transfer rate constant k_s was estimated to be 46.8 s^{-1} according to the formula $m = (RT/F)\,(k_s/n\nu)$. The transfer coefficient α was taken as 0.5, and one electron for the heme group, m for CYP1A1 in this work is 1.2 according to Laviron (1979). The symbols R, T and F have their usual electrochemical meanings. In the NADPH-dependent cytochrome p450 s catalytic reaction in microsomal system the rates of substrate binding with cytochrome p450 and the following reduction of cytochrome p450 were 50 and 18 s^{-1}, respectively (Lewis, 1996). In the present work, the electron transfer rate constant k_s of 46.8 s^{-1} is comparable with the native cytochrome p450s catalytic system, thus it is suitable for the cytochrome p450s catalytic reaction.

The pH of buffer solutions had significant influence on CV peak potentials of CYP1A1-*nano-SWy-2*-DHP film. Both reduction and oxidation peaks shifted negatively with increasing pH (inset in Fig. 3). In the pH range studied from 2 to 10, E_{pa}, E_{pc} and $E_{0'}$ shifted to the negative direction with a slope of 55 mV pH^{-1}, 52 mV pH^{-1} and 50 mV pH^{-1}, respectively. All values are smaller than the theoretically expected value of 59 mV pH^{-1} for the transfer of one proton and one electron per heme group during the electrode reaction (Bond, 1980), indicating that a single protonation accompanies the electron transfer of P-FeIII to the electrodes. Thus, the simplified equation for the reduction of P-FeIII of CYP1A1 in *nano-SWy-2*-DHP film can be depicted as:

$$\text{P-FeIII} + \text{H}^+ + \text{e}^- \leftrightarrow \text{P-FeII}$$

The pH value does also affect on CV peak currents of CYP1A1-*nano-SWy-2*-DHP film. It was found that the maximum peak currents are observed at pH 7.0. It may be due to the immobilized CYP1A1 maintains its higher bioactivity at pH 7.0. Thus, pH 7.0 was selected in this experiment to obtain better signal.

3.3. Catalytic activity of CYP1A1 in nano-SWy-2-DHP film

Electrocatalytic reduction of oxygen by CYP1A1-nano-SWy-2-DHP film was investigated by cyclic voltammetry (Fig. 4). When

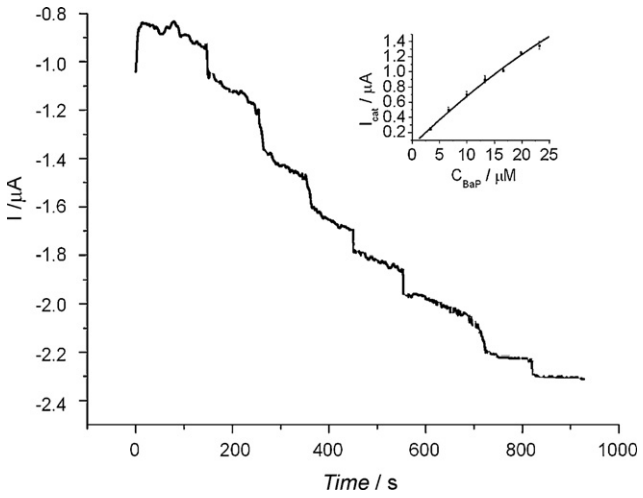

Fig. 5. Electrochemical responses at CYP1A1-nano-SWy-2-DHP/EPG at −0.45 V in 12 mL of the pH 7.0 air-saturated buffer with injecting 10 μL of 3.96 mM benzo[*a*]pyrene every 100 s. Inset in Fig.5: calibration curve of the reduction peak currents vs. the concentration of benzo[*a*]pyrene.

a certain amount of air was injected into a pH 7.0 buffer solutions by a syringe, a marked increased in reduction peak at about −0.38 V was observed for CYP1A1-nano-SWy-2-DHP film. However, direct reduction of O_2 was observed at nano-SWy-2-DHP film at the potential −0.8 V. These results are characteristics of catalytic reduction O_2 by CYP1A1 confined in nano-SWy-2-DHP film.

B[a]P is a potent carcinogen, and widely spread in the environment. To develop a simple, general purpose B[a]P sensor that directly detects B[a]P is of significance. Here, the electrocatalytic oxidation of B[a]P was examined by cyclic voltammetry with CYP1A1-nano-SWy-2-DHP film (Fig. 4). The electrocatalytic efficiency of CYP1A1 to the B[a]P oxidation at the CYP1A1-nano-SWy-2-DHP/EPG was investigated based on the value of i_{cat}/i_d (where i_d and i_{cat} are the cathodic steady-state current before and after adding B[a]P, respectively) on the applied voltage. In the presence of 10 μM B[a]P in pH 7.0 phosphate buffer, the ratio of i_{cat}/i_d gradually increased with decreasing negatively applied voltage from 0 to −0.45 V and exhibited a maximum value at −0.45 V. However, i_{cat}/i_d decreased when the applied voltage was higher than −0.45 V. Thus, a working voltage of −0.45 V was chosen for the amperometric determination of B[a]P. When B[a]P was added to 10 mL pH 7.0 buffer, an increase of P-FeIII reduction peak at about −0.38 V was observed, accompanied by a decreased of P-FeII oxidation. The reduction peak current increased with the concentration of B[a]P. These results indicated that a cycle catalytic reaction between P-FeII and B[a]P occurred and produced P-FeIII and hydroxylated B[a]P again (Denisov et al., 2005). The catalytic mechanisms can be expressed as the follows:

$$\text{CYP1A-FeII} + \text{B[a]P} \rightarrow \text{CYP1A-FeIII} + \text{hydroxylated B[a]P}$$

$$\text{CYP1A-FeIII} + \text{e(supplied by electrode)} \rightarrow \text{CYP1A-FeII}$$

The current response of CYP1A1-nano-SWy-2-DHP film to B[a]P was also studied by amperometric $i \sim t$. A current–time response of CYP1A1 on 7 successive step changes of B[a]P concentration is shown in Fig. 5. With the selected working potential −0.45 V, when an aliquot of B[a]P is added into the buffer solution, the reductive current increases and reaches the steady-state within 50 s, which indicates a fast diffusional process and a high activity of CYP1A1 in nano-SWy-2-DHP film. The calibration range of B[a]P is from 3.312–16.56 μM, a sensitivity of 58.57 μA mM^{-1} and an intercept of 0.09 μA with a correlation coefficient, *r*, of 0.996. The detection limit was estimated to be 0.58 μM. The sensor showed good reproducibility for the determination of B[a]P concentration in the linear range. The variation coefficient was 3.5% for 7 successive assays of 6.624 μM B[a]P. The stability tests were carried out at room temperature by measuring the response from day to day and the CYP1A1 biosensor was kept at room temperature. It was shown that the biosensor maintains its 87% initial activity after 10 days.

When the concentration of B[a]P in the electrochemical cell was higher than 16.6 μM, a plateau was observed, showing a characteristic of the Michaelis–Menten kinetic mechanism. The apparent Michaelis–Menten constant, K_m^{app}, which becomes a measure of the affinity of an enzyme for its substrate, can be obtained from the electrochemical version of the Lineweaver–Burk equation:

$$\frac{1}{I_{ss}} = \frac{1}{I_{max}} + \frac{K_m^{app}}{I_{max}C}$$

Here, I_{ss} is the steady-state current after the addition of substrate, *C* is the bulk concentration of the substrate, and I_{max} is the maximum current measured under saturated substrate conditions. The K_m^{app} value for the CYP1A1-*nano-SWy-2*-DHP/EPG was found to be 46.27 μM [I^{-1} (μA) = 0.84 + 38.87C^{-1} (μM), $R = 0.997$, $n = 5$], which are about two-fold larger than that for the native NADPH-supported value 19 μM determined by HPLC method (Chun et al., 1996). And it is indicated that the affinity of CYP1A1, which immobilized in *nano-SWy-2*-DHP film, is slightly decreased.

4. Conclusions

In this work, high-level expression of full-length rat cytochrome p450 1A1 can be achieved in *E. coli* using NH_2-terminal fusions with bacterial signal peptides *ompA*. The expressed enzyme has been found to be spectrally active, functional protein. Sufficient amounts of cytochrome p450 1A1 were collected from the membrane fractions of *E. coli* and were immobilized in nano-SWy-2-DHP film to develop a biosensor. The catalytic behavior of the CYP1A1 biosensor to its substrate benzo[*a*]pyrene was investigated by voltammetry and amperometry. The calibration range of benzo[*a*]pyrene is from 3.31–16.56 μM with a detection limit 0.58 μM. And this biosensor was found to show good reproducibility and stability.

Acknowledgements

The project was financed by the National Natural Science Foundation of China (Nos. 20777094 and 30771163) and partially financed by Academic Innovation Team for Plant Development and Genetics in South-Central University for Nationalities (XQ Liu group).

References

Akpan, V., Lodovici, M., Dolare, P., 1994. Bull. Environ. Contam. Toxicol. 53, 246–253.
Bond, A.M., 1980. Modern Polarographic Methods in Analytical Chemistry. Marcel Dekker, New York, pp. 27–45.
Chun, Y.J., Shimada, T., Guengerich, F.P., 1996. Arch. Biochem. Biophys. 330, 48–58.
Chung, J.Y., Kim, J.Y., Kim, W.R., Lee, S.G., Kim, Y.J., Park, J.E., Hong, Y.P., Chun, Y.J., Park, Y.C., Oh, S., Yoo, K.S., Yoo, Y.H., Kim, J.M., 2007. Toxicology 235, 62–72.
Denisov, I.G., Makris, T.M., Sligar, S.G., Schlichting, I., 2005. Chem. Rev. 105, 2253–2277.
Guo, Z.Y., Gillam, E.M.J., Ohmori, S., Tukey, R.H., Guengerich, F.P., 1994. Arch. Biochem. Biophys. 312, 317–589.
Hecht, S.S., 1999. J. Natl. Cancer Inst. 91, 1194–1210.
Ji, Y.K., Chung, J.Y., Park, J.E., Lee, S.G., Kim, Y.J., Cha, M.S., Han, M.S., Lee, H.J., Yoo, Y.H., Kim, J.M., 2007. Endocrinology 148, 5112–5122.
Larson, J.R., Coon, M.J., Porter, T.D., 1991. J. Biol. Chem. 266, 7321–7324.
Laviron, E., 1979. J. Electroanal. Chem. 101, 19–28.
Lewis, D.F.V., 1996. Cytochrome p450. Structure, Function and Mechanism. Taylor and Francis, London.
Lowry, O.H., Rosebrough, N.J., Farr, A.L., Randell, R.J., 1951. J. Biol. Chem. 193, 265–275.
Monteilhet, C., Lachacinski, N., Aggerbeck, L.P., 1993. Gene 125, 223–228.

Murray, R.W., 1984. In: Bard, A.J. (Ed.), Electroanalytical Chemistry, Vol. 13. Marcel Dekker, New York, pp. 191–368.
Omura, T., Sato, R., 1964. J. Biol. Chem. 239, 2370–2378.
Pacifici G.M., Fracchia G.N.,;1; 1995. Medicine and health. In Advances in Drug Metabolism in Man. EUR 15439. Luxembourg: Office for Official Publications of the European Communities, pp. 179-231.
Pritchard, M.P., Ossetian, R., Li, D.T.N., Henderson, C.J., Burchell, B., Wolf, C.R., Friedberg, T., 1997. Arch. Biochem. Biophys. 345, 342–354.
Sandhu, P., Guo, Z.Y., Baba, T., Martin, M.V., Tukey, R.H., Guengerich, F.P., 1994. Arch. Biochem. Biophys. 309, 168–177.
Shimada, T., Yun, C.H., Yamazaki, H., Gautier, J.C., Beaune, P.H., Guengerich, F.P., 1992. Mol. Pharmacol. 41, 856–864.
Shimada, T., 2006. Drug Metab. Pharmacokinet. 21, 257–276.
Solhaug, A., Refsnes, M., Lag, M., Schwarze, P.E., Husoy, T., Holme, J.A., 2004. Carcinogenesis 25, 809–819.
Troche, S.V., García Falcón, M.S., Amigo, S.G., Yusty, M.A.L., Lozano, J.S., 2000. Talanta 51, 1069–1076.
Uno, S., Dalton, T.P., Dragin, N., Curran, C.P., Derkenne, S., Miller, M.L., Shertzer, H.G., Gonzalez, F.J., Nebert, D.W., 2006. Mol. Pharmacol. 69, 1103–1114.
Yuan, S., Chen, W.H., Hu, S., 2004. Talanta 64, 922–928.
Zhang, L., Liu, X.Q., Wang, C.T., Liu, X.Q., Cheng, G., Wu, Y.H., 2010. Protein Exp. Purif. 71, 74–78.
Zhao, X.J., Mai, Z.B., Kang, X.H., Zou, X.Y., 2008. Biosens. Bioelectron. 23, 1032–1038.
Zhou, Y.L., Hu, N.F., Zeng, Y.H., Rusling, J.F., 2002. Langmuir 18, 211–219.